DOI: 10.26599/FSHW.2026.9251049

Contents lists available at SciOpen

Food Science and Human Wellness

journal homepage: https://www.sciopen.com/journal/2097-0765

China Food Publishing Co.

Mangiferin alleviates oxidative stress and modulates the inflammatory microenvironment in oligospermia by regulating pyroptosis

Yahong Cheng[a,e,1], Zhenjiang Hou[c,1], Minghan Lu[a,b,1], Yuliang Peng[e], Jinhu Zhang[e], Minghui Wang[d], Xu Cao[e], Mei Ke[e], Yang Pu[e], Chaofan Liu[e], Ning Chen[d,*], Ming Zhang[a,b,*], Junhao Lei[a,b,*]

[a] *Center for Reproductive Medicine, Zhongnan Hospital of Wuhan University, Wuhan, Hubei 430071, China*

[b] *Clinical Medicine Research Centre of Reproductive Health and Birth Health in Wuhan City, Wuhan, Hubei 430071, China*

[c] *Department of Urology, Shache County People's Hospital, Kashgar, Xinjiang 844000, China*

[d] *Tianjiu Research and Development Center for Exercise Nutrition and Foods, Hubei Key Laboratory of Exercise Training and Monitoring, College of Sports Medicine, Wuhan Sports University, Wuhan 430079, China*

[e] *College of Medicine and Health Science, Wuhan Polytechnic University, No.68, Xuefu South Road, Wuhan, Hubei 430023, China*

ABSTRACT: Oligospermia (OA) represents a significant contributor to male infertility, with a pressing need for effective and low-side-effect therapeutic strategies. This study aims to investigate the ameliorative effects of mangiferin (MG) on OA and its underlying molecular mechanisms. To this end, an OA rat model was induced using busulfan (BU), wherein the effects of MG on sperm quality, testis histopathology, and serum hormone levels were assessed. Furthermore, an *in vitro* model of testicular Sertoli cells was prepared using benzimidazole (DRB) to evaluate the impact of MG on cell viability and apoptosis. Integrative bioinformatics approaches predicted targets and pathways associated with MG, supplemented by molecular docking and validation experiments employing Western blot and RT-qPCR techniques to elucidate the regulation of the NLRP3-ASC-Caspase-1-GSDMD signaling pathway. Results demonstrated that MG significantly enhanced sperm quality and rescued testicular tissue damage in OA rats while restoring hormonal balance. *In vitro* experiments corroborated these findings by showing increased Sertoli cell viability and reduced apoptosis. Network pharmacology and enrichment analysis indicated that MG exerts its effects primarily by inhibiting NLRP3 inflammasome activation. Mechanistic investigations revealed that MG downregulated the expression of NLRP3, ASC, Caspase-1, and GSDMD, thereby suppressing pyroptosis while mitigating oxidative stress (lowering MDA and enhancing SOD) and inflammatory responses (reducing TNF-α and IL-1β). In conclusion, MG regulates cell pyroptosis *via* the NLRP3-ASC-Caspase-1-GSDMD axis, thereby mitigating oxidative stress and modulating the inflammatory microenvironment in OA, suggesting its potential as a promising therapeutic agent for male infertility.

Keywords: Oligospermia; mangiferin; pyroptosis; NLRP3-ASC-Caspase-1-GSDMD pathway

1. Introduction

The global incidence of male infertility is on the rise due to various factors, including increasing work burdens, employment pressures, genetic predispositions, psychological stress, poor dietary habits, and

[1] These authors contributed equally to this work and should be considered co-first authors.
*** Corresponding authors.**
Lei_junhao@163.com, Ming Zhang, whu_mz@163.com, nchen510@gmail.com.

Received 28 June 2025
Received in revised from 15 September 2025
Accepted 31 December 2025

environmental pollution[1–4]. According to data from the World Health Organization (WHO), infertility affects approximately 20% of reproductive-aged couples, with male factors contributing to 40–60% of these cases—a proportion that is increasing annually. Abnormal semen parameters are responsible for 70–80% of male infertility cases, with oligospermia (OA) accounting for approximately 10% of these. Alarmingly, human sperm counts are declining at an annual rate of 1%, indicating a progressive deterioration in testicular spermatogenic function. Current therapeutic approaches, including pharmacotherapy, surgery, and assisted reproductive technologies (ART)[5–7], face significant limitations. Pharmacological treatments demonstrate variable efficacy due to individual differences and adverse effects that compromise the quality of life, while they often lack etiology-specific targeting. Surgical interventions may be beneficial in select cases, but they carry high risks and require prolonged recovery, imposing substantial physical and psychological burdens on patients[8]. Although ART, such as in *vitro* fertilization, can assist certain patients, it remains financially burdensome, and success rates are influenced by multiple factors multiple factors influence success rates. Consequently, the suboptimal efficacy of current therapies highlights the urgent need to elucidate OA's pathogenesis and develop novel interventions. Such advancements are essential for delivering effective treatments and improving fertility outcomes and quality of life for affected individuals.

The core pathological basis of OA lies in testicular injury, primarily driven by the synergistic effects of oxidative stress and inflammation. Oxidative stress impairs sperm function through excessive reactive oxygen species (ROS), inducing sperm membrane lipid peroxidation, DNA fragmentation, and protein oxidation, ultimately reducing sperm motility and fertilization capacity[9]. Concurrently, elevated inflammatory cytokines, such as IL-1β, IL-6, and TNF-α, in the testicular microenvironment disrupt the blood-testis barrier (BTB) and impair spermatogenic cell proliferation. Notably, oxidative stress and inflammation form a vicious cycle, mutually reinforcing each other and exacerbating testicular damage and dysfunction[10]. Studies demonstrate that NADPH oxidase inhibition reduces ROS accumulation, thereby attenuating inflammation and suppressing NLRP3 inflammasome activation, highlighting a promising therapeutic strategy.

Pyroptosis, an inflammasome-mediated programmed cell death mechanism, exacerbates tissue damage by releasing pro-inflammatory cytokines and ROS[11]. Research indicates that testicular spermatogenic cells undergo pyroptosis under oxidative stress and inflammatory stimuli, leading to structural disintegration of the seminiferous epithelium and significant declines in sperm count[12]. Activation of pyroptosis-associated proteins such as GSDMD-N induces cell membrane pore formation, which results in the release of inflammatory mediators including IL-1β and IL-18[13]; these mediators recruit immune cell infiltration, perpetuating a pro-inflammatory microenvironment that contributes to extensive germ cell loss in OA patients[14,15].

The NLRP3 inflammasome is a central molecular switch linking oxidative stress to pyroptosis. In OA models, toxic agents such as busulfan[16] trigger NLRP3 inflammasome assembly by inducing K^+ efflux, ROS accumulation, and lysosomal rupture. Activated NLRP3 recruits Caspase-1 *via* ASC, which cleaves pro-IL-1β and pro-IL-18 into their active forms and processes GSDMD into the pore-forming GSDMD-N

fragment, thereby driving pyroptosis[17]. Additionally, NLRP3 activation promotes ROS generation through positive feedback loops, further exacerbating oxidative stress[18]. Notably, inhibition of the NLRP3 pathway has been shown to significantly reduce testicular cell pyroptosis and improve spermatogenesis, highlighting its therapeutic potential[19,20].

Mangiferin (MG), a polyphenolic bioactive compound predominantly found in mangoes, has garnered significant attention as a potential dietary supplement due to its multifaceted biological activities, including potent antioxidant, anti-inflammatory, and anti-apoptotic properties. Emerging research highlights the role of dietary supplements in mitigating testicular damage and enhancing spermatogenesis. For instance, Yu et al. [21] demonstrated that sea cucumber-derived male gonad peptides exert testicular protective effects by suppressing inflammatory responses and promoting spermatogenesis. Similarly, MG has been shown to alleviate oxidative stress by modulating intracellular antioxidant enzyme activity [22]. Nevertheless, the therapeutic efficacy of mangiferin in oligospermia remains unexplored. In this study, we first investigated the therapeutic potential of mangiferin in an OA animal model, then predicted its molecular targets using network pharmacology, and finally validated the underlying mechanisms through *in vitro* experiments. Our findings revealed that MG possesses robust antioxidant activity and ameliorates reproductive function by suppressing germ cell pyroptosis by inhibiting the NLRP3-ASC-Caspase-1-GSDMD signaling pathway, effectively attenuating inflammatory responses and oxidative damage.

2. Materials and methods

2.1 Drugs and reagents

Mangiferin (MG, purity ≥98% [HPLC], Cat. No. M875869) and busulfan (BU) (Cat. No. B803921) were purchased from Macklin Inc. (Shanghai, China), and sodium carboxymethyl cellulose (CMC-Na) (Cat. No. 30036365) was obtained from China National Pharmaceutical Group Corp. (Beijing, China).

2.2 Animals

A total of sixty healthy male Sprague-Dawley (SD) rats, aged 8 weeks and weighing 250-280g, were procured from Yizhicheng Biotechnology Co., Ltd. (Animal License No.: SYXK 2022-0124). Upon arrival, the animals underwent a one-week acclimatization period. They were housed in a SPF facility, where conditions were strictly controlled at a temperature of 24-26°C and a relative humidity of 50-60%, with a 12-hour light/dark cycle. All rats had ad libitum access to a standard rodent diet and sterilized water throughout the experimental period. This experimental protocol was approved by the Ethics Committee of Wuhan Polytechnic University (Approval No. BME-2024-2-14) and strictly adheres to the ARRIVE (Animal Research: Reporting of In Vivo Experiments) guidelines, the National Institutes of Health (NIH) Guidelines for the Care and Use of Laboratory Animals and the breeding standards for rodents, so as to maximize animal welfare.

2.3 Establishment of busulfan-induced oligospermia (OA) rat model and MG intervention

Sixty rats were randomly assigned to seven groups (n=10 per group): (1) blank control, (2) busulfan-induced model, (3–5) mangiferin treatment (15, 30, and 60 mg/kg) [23], and (6) vitamin E positive control (100 mg/kg) [24]. The grouping was performed using a random number table method. Specifically, all rats were numbered according to their body weights, and random numbers were generated to assign them into different groups, ensuring comparable average body weights and baseline conditions across groups. Oligospermia was induced by intraperitoneal injection of busulfan (3 mg/kg in saline) for five consecutive days. Subsequently, mangiferin and vitamin E were administered daily for 30 days via oral gavage, suspended in 0.5% CMC-Na.

2.4 Body weight monitoring and testis index assessment

Body weight was measured every 3 days, and general health status (e.g., fur condition, activity level) was monitored. 24 h after the final treatment, rats were anesthetized with 1% sodium pentobarbital (50 mg/kg, i.p.) (Sigma-Aldrich, Shanghai, China, Cat. No. P3761). Blood samples were collected *via* cardiac puncture, followed by euthanasia. Testes were promptly excised and weighed, and the testis index was determined as testis weight (mg) relative to body weight (g) (expressed as mg/g).

2.5 Evaluation of sperm count, motility, and deformity rate

Sperm samples were obtained from the caudal epididymis. For quantitative analysis, a 10 μL aliquot of sperm suspension was placed on a hemocytometer, and sperm concentration and progressive motility were evaluated under a microscope at 200× magnification. For morphological assessment, an additional 10 μL aliquot was stained with Diff-Quik solution (Solarbio Science & Technology Co., Ltd., Beijing, Cat. No. G1541), and sperm abnormalities were examined according to standardized criteria.

2.6 Histopathological evaluation of testicular tissue by Hematoxylin-Eosin (H&E) staining

Testicular tissue samples were fixed in 4% paraformaldehyde for 24h at 4°C. Following fixation, tissues were processed through a graded ethanol series (70%-100%) for dehydration, cleared in xylene, and embedded in paraffin. Sections (4 μm thick) were cut using a microtome, mounted on glass slides, and dried overnight at 37°C. For staining, sections were deparaffinized in xylene, rehydrated through graded alcohols, and stained with hematoxylin (5 min) followed by eosin (2 min). After dehydration and clearing, slides were covered with neutral balsam. Histopathological examination was performed under a light microscope at 200× magnifications.

2.7 Serum sex hormone analysis

Whole blood samples obtained via cardiac puncture from anesthetized rats were incubated at room temperature for 2 h to allow complete clotting. The serum was subsequently separated by centrifugation at 3500 × g for 20 min at 4°C. The concentrations of follicle-stimulating hormone (FSH), luteinizing hormone (LH), and testosterone (T) were determined in the serum using commercially available ELISA kits according to the manufacturer's protocols.

2.8 Network pharmacology analysis of mangiferin's mechanism of action

2.8.1 Identification of drug and disease targets

MG Potential targets were predicted using three bioinformatics platforms: SwissTargetPrediction, TargetNet, and SuperPred. After removing duplicates, a set of candidate targets was obtained. Concurrently, OA-related targets were retrieved from four databases (GEO, GeneCards, OMIM, and CTD). Duplicates among the disease targets were also removed to compile a non-redundant list of OA-associated targets.

2.8.2 Identification of drug-disease common targets

The intersection between MG's potential targets and OA-related targets was analyzed using Venn 2.1.0, yielding overlapping targets representing potential therapeutic interactions.

2.8.3 Construction of protein-protein interaction (PPI)

PPI data for the overlapping targets were retrieved from the STRING database, with interactions filtered at a high-confidence threshold (combined score $\geq$ 0.700). The network was constructed and visualized using Cytoscape 3.10.0. Core targets among the overlapping targets were identified based on topological analysis of degree centrality, closeness centrality, and betweenness centrality. Additionally, the CytoHubba plugin with the Maximal Clique Centrality (MCC) algorithm was applied to further identify hub genes.

2.8.4 Functional enrichment analysis

The overlapping targets were analyzed using the DAVID database for GO functional annotation (including biological processes [BP], molecular functions [MF], and cellular components [CC]) and KEGG pathway enrichment analysis, with all analyses performed through the Weishengxin bioinformatics platform.

2.8.5 Molecular docking validation

The two-dimensional structure of MG was obtained from PubChem and converted to its three-dimensional conformation using Chem3D. Following hydrogenation in AutoDockTools 1.5.7, the ligand was prepared in PDBQT format. Crystal structures of core target proteins were retrieved from the PDB with the following selection criteria: (1) Homo sapiens origin, (2) X-ray diffraction method, (3) resolution $\leq$2.5 Å, and (4) publication between 2020-2025. PyMOL 2.5 removed water molecules and non-essential ligands from the protein structures. The receptor proteins were then processed in AutoDockTools 1.5.7 by adding polar hydrogens and converting them to PDBQT format. Molecular docking was performed using AutoDock Vina 4.2. Result visualization and analysis were conducted with PyMOL 2.5 and Discovery Studio 2019.

2.9 Sertoli cell culture

Primary Sertoli cells isolated from Sprague-Dawley rat testes (Shangen Biotechnology, Cat. No.: SNP-R071) were cultured in DMEM supplemented with 10% FBS and 1% penicillin-streptomycin (100 U/mL penicillin and 100 μg/mL streptomycin). Cells were maintained at 37°C in a humidified atmosphere containing 5% CO_2.

2.10 Establishment of in vitro OA model and pharmacological interventions

An *in vitro* model of oligospermia was established by treating Sertoli cells with 1000 μg/mL benzimidazole (DRB) [25,26] (Sigma-Aldrich, Shanghai, China, Cat. No. D1916) for 24 h, followed by 24-h recovery in normal medium. For drug intervention studies, DRB-pretreated cells were exposed to MG at concentrations ranging from 25 to 400 μg/mL (25, 50, 100, 200, and 400 μg/mL) for 24 h. Control groups were untreated Sertoli cells maintained in a normal culture medium throughout the experimental period.

2.11 CCK-8 assay

Cells were seeded in 96-well plates at a density of 1×10^3 cells per well and allowed to adhere for 24 h. Following the treatment protocols described in Section 2.10, each experimental group was assayed with six replicate wells. Additionally, a separate set of cells was treated with a gradient concentration of mangiferin and benzimidazole (DRB) specifically for IC50 calculation. After treatment, the medium was carefully aspirated and replaced with 100 μL of fresh medium containing 10% (v/v) CCK-8 reagent. The plates were incubated at 37°C in a light-protected environment for 1 h. Absorbance was measured at 450 nm using a microplate reader. In addition, the calculated IC50 value and the corresponding dose-response curve are provided in Supplementary Figure 1.

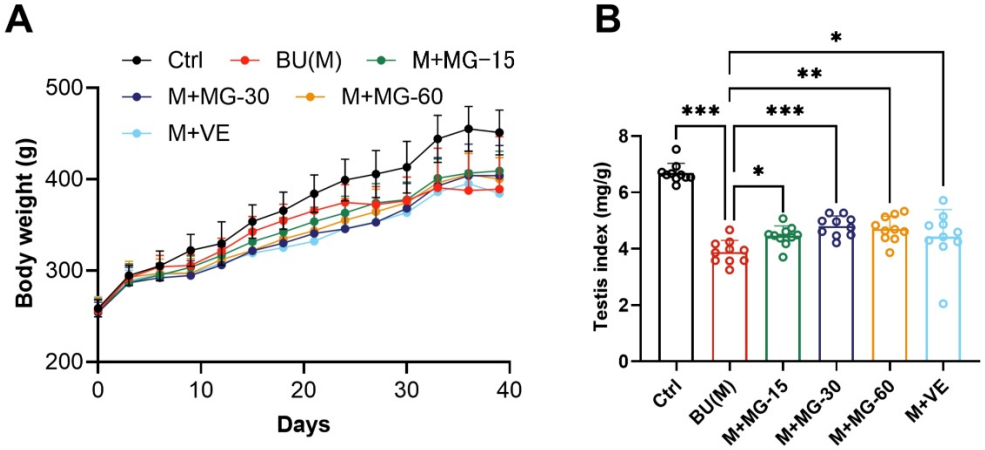

Figure 1. Mangiferin (MG) attenuated weight loss and improved testis index in oligospermia (OA) rats. (A) Body weight and (B) testis index were monitored. The testis index was calculated as the ratio of testis weight to body weight at dissection. Data were presented as Mean ± SD (n = 10). **P* < 0.05, ***P* < 0.01, ****P* < 0.001.

2.12 Hoechst 33342 staining

Cells cultured on coverslips in 6-well plates were washed twice with PBS and fixed with 4% paraformaldehyde for 15 min at room temperature. After PBS washing, cells were stained with 0.5 mL Hoechst 33342 solution (10 μg/mL in PBS) for 25 min at room temperature in the dark. Following three 5-minute PBS washes, coverslips were mounted using an antifade mounting medium and visualized under an inverted fluorescence microscope.

2.13 Measurement of oxidative stress biomarkers

For tissue analysis, testicular samples (100 mg) were homogenized in ice-cold PBS (1:9, w/v) using a tissue homogenizer. The homogenates were centrifuged at 5000 × g for 15 min at 4°C, and the supernatants were aliquoted for analysis. For cellular analysis, Sertoli cells (5×10^6 cells/well) were cultured in 6-well plates. Following treatment, cells were washed with ice-cold PBS and lysed with RIPA buffer containing

protease inhibitors. The supernatants were collected after centrifugation at 12,000 × g for 15 min at 4°C. Protein concentrations were determined by using a BCA protein assay. Oxidative stress markers, including malondialdehyde (MDA), superoxide dismutase (SOD), and glutathione peroxidase (GSH-Px) activities, were measured using commercial assay kits according to manufacturers' protocols.

2.14 Quantification of inflammatory cytokines

Both testicular tissue homogenates and Sertoli cell lysates were centrifuged at 12,000 × g for 15 min at 4°C to obtain clear supernatants. Total protein concentration was determined using the BCA protein assay. The concentrations of pro-inflammatory cytokines (TNF-α, IL-1β, and IL-6) and anti-inflammatory cytokine (IL-10) were measured in both supernatants using commercially available ELISA kits according to the manufacturer's instructions.

2.15 Western blot

Cell lysates were centrifuged at 12,000 × g for 15 min at 4°C, and protein concentrations were determined by BCA assay. Equal amounts of protein (50 μg) were separated on 10% SDS-PAGE and transferred to PVDF membranes using a wet transfer system. Membranes were blocked with 5% non-fat milk in TBST for 2 hours at room temperature, followed by incubation with primary antibodies overnight at 4°C, including anti-NLRP3 (Rabbit, Proteintech, Beijing, China, Cat. No. 30109-1-Ap), anti-Caspase-1 (Rabbit, ZENBIO, Chengdu, China, Cat. No. 342947), anti-GSDMD (Rabbit, Affinity, Chengdu, China, Cat. No. AF4012), and anti-β-actin (Rabbit, BIOSS, Beijing, China, Cat. No. BS-0061R) at 1:1000 dilution. After washing with TBST (3 × 10 min), membranes were incubated with HRP-conjugated goat anti-rabbit secondary antibody (Abcam, Cambridge, UK, No. ab205718) at a 1:4000 dilution for 1 hour at room temperature. Protein bands were detected using an ECL substrate and quantified using ImageJ software after image acquisition with an AI600 imaging system.

2.16 RT-qPCR

Total RNA was extracted from testicular tissues or cell samples using an RNA extraction kit. The concentration and purity of RNA were measured by UV spectrophotometry. Following the manufacturer's instructions for the cDNA synthesis kit, cDNA was synthesized from RNA templates by adding reverse transcriptase and specific primers. For RT-qPCR, the reaction began with an initial denaturation at 95°C for 10 min, followed by 45 cycles of denaturation at 95°C for 15 sec and annealing/extension at 60°C for 1 min. β-actin was used as the internal reference gene, and the relative expression of target genes was calculated using the $2^{-\Delta\Delta Ct}$ method. Primer sequences are provided in Supplementary Table 1.

2.17 Targeted energy metabolism metabolomics

2.17.1 Sample Preparation

Testicular tissue samples from SD rats were used for targeted energy metabolism metabolomics analysis. Approximately 50 mg (±2.5 mg) of each sample was accurately weighed into a 2 mL centrifuge tube. Immediately, 500 μL of pre-chilled (−20°C) 70% methanol aqueous solution was added, followed by 3

min vortex mixing. After centrifugation at 12,000 × g for 10 min at 4°C, 300 μL of supernatant was transferred to a 1.5 mL tube and stored at −20°C for 30 min. The samples were then recentrifuged under identical conditions. Finally, 200 μL of supernatant was filtered through a protein precipitation plate and stored at −20°C before LC-MS analysis.

2.17.2 Chromatographic and mass spectrometric conditions

Chromatographic separation was achieved using an ACQUITY UPLC BEH Amide column (1.7 μm, 100 × 2.1 mm) maintained at 40°C. The binary mobile phase consisted of (A) 10 mM ammonium acetate and 0.3% ammonia in ultrapure water and (B) acetonitrile/water (90:10, v/v), delivered at 0.40 mL/min with the following gradient program: 5% A (0-1.2 min), linear increase to 30% A (8.0 min), 50% A (9.0-11.0 min), and re-equilibration to initial conditions (11.1-15.0 min). The injection volume was 2 μL.

Mass spectrometric detection was performed using a Q-Trap® 6500+ system with an electrospray ionization source operated at 550°C in positive (5500 V) and negative (-4500 V) ion modes. The curtain gas was maintained at 35 psi. Optimized declustering potentials and collision energies were established for each analyte through individual ion pair optimization.

2.17.3 Data processing and analysis

Mass spectrometry data were processed using Analyst 1.6.3 and MultiQuant 3.0.3 software. Chromatographic peaks were integrated and retention time-aligned using reference standards to ensure accurate identification and quantification.

Multivariate statistical analysis was performed in R software (version 4.3.1). PCA was conducted using the prcomp function with unit variance scaling. OPLS-DA was implemented through the MetaboAnalyst R package.

Differential metabolite screening employed a two-tiered approach: (1) preliminary selection based on VIP scores (VIP >1) from OPLS-DA models (n≥3 biological replicates), followed by (2) confirmation using univariate analysis (*P*-value/FDR <0.05 and |log2FC|≥1, n≥2 biological replicates). Metabolites meeting both criteria were considered significantly differentially expressed.

2.18 Statistical analysis

Data analysis and visualization were performed using SPSS 25.0 and GraphPad Prism 10.1.2. Continuous variables were presented as Mean ± SD. Body weight differences between groups were analyzed by two-way ANOVA, while other parameters were compared using one-way ANOVA. Post hoc pairwise comparisons were conducted with Fisher's LSD test. A threshold of $P < 0.05$ was considered statistically significant. Data were tested for normality and homogeneity of variances using the Shapiro–Wilk test and Levene's test, respectively. The results of these tests are provided in Supplementary Table 2.

3. Results

3.1 Therapeutic effects of mangiferin (MG) in an oligospermia (OA) rat model

3.1.1 MG ameliorated body weight loss and testicular atrophy

To evaluate the therapeutic potential of MG, we monitored body weight dynamics and calculated the testis index (testis-to-body weight ratio) in OA model rats. All groups showed initial weight gain followed by stabilization, but the model group exhibited significantly attenuated weight gain from day 9 onward compared to normal controls. While MG-treated groups initially mirrored the model group's weight pattern, extended treatment (30 days) significantly prevented weight loss versus the model group. The vitamin E (VE) positive control showed marginal effects on body weight (Figure 1A and Supplementary Table 3).

The model group displayed significant testicular atrophy (reduced testis index versus controls, $P < 0.001$), which was markedly reversed by MG treatment (Figure 1B). These results demonstrate that MG effectively counteracts systemic metabolic impairment and testicular dysfunction in OA.

3.1.2 MG attenuated busulfan-induced sperm quality impairment in OA rats

The defining pathological feature of OA is a systemic deterioration in sperm quality. This study comprehensively assessed the therapeutic effects of MG on sperm concentration, motility, and deformity rate (Figure 2A-D). Results showed that busulfan-induced OA model rats exhibited significantly impaired sperm motility, a declining sperm concentration trend, and increased deformity rate, aligning with OA characteristics. MG treatment at all doses (15, 30, and 60 mg/kg) markedly restored sperm concentration and motility while reducing deformity rates. Dose-response analysis revealed comparable efficacy in improving sperm concentration and motility across dose groups. However, the 30 and 60 mg/kg groups outperformed the 15 mg/kg group in ameliorating sperm deformity rates. In contrast, VE (positive control) only significantly reduced the deformity rate without notable effects on other parameters. These findings conclusively demonstrate MG's multifaceted reproductive protective effects, enhancing sperm quantity (concentration) and quality (motility and morphology).

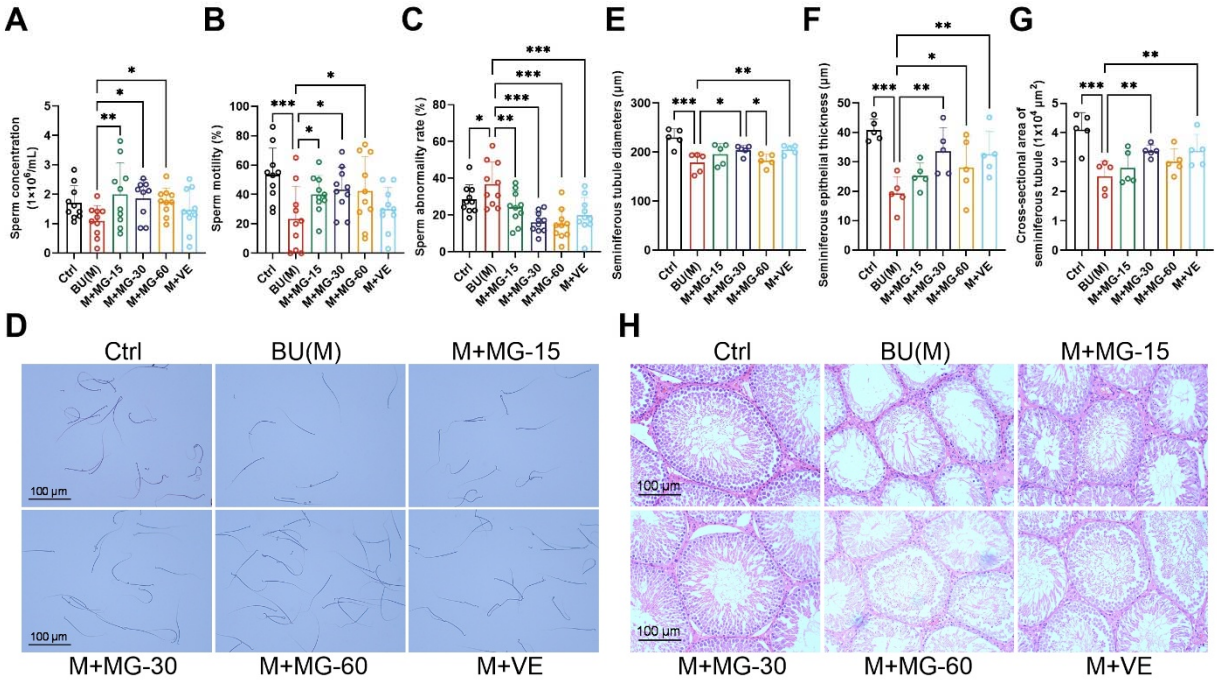

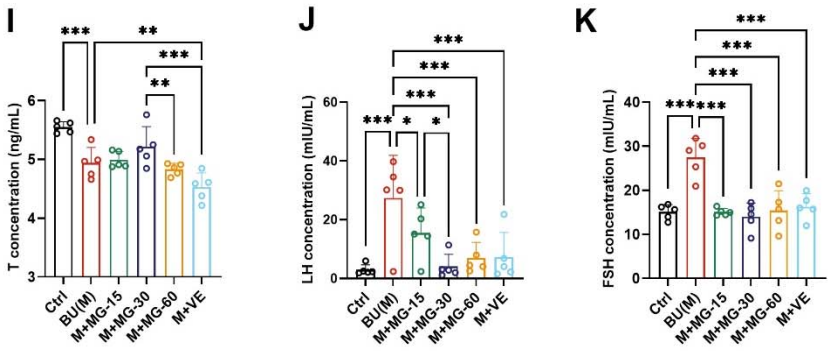

Figure 2. The ameliorative effects of MG on sperm quality, testicular pathology, and hormone levels in OA rats. (A) Sperm concentration and (B) sperm motility were detected in epididymal sperm. (C) Sperm abnormality rate was observed by Diff staining. (D) Representative images of Diff staining of sperm from each group. (E) Testicular tissue damage observed by HE staining, with (F) diameter of seminiferous tubules, (G) thickness of seminiferous tubule epithelium, and (H) cross-sectional area of seminiferous tubules calculated. (I) Representative images of HE staining of testicular tissue. (J) Serum T, (K) LH, and (L) FSH levels were detected. Scale bars: 100 μm. Data were presented as Mean ± SD (n=10 for sperm parameters, n=5 for others). **P* < 0.05, ***P* < 0.01, ****P* < 0.001.

3.1.3 MG mitigated busulfan-induced testicular damage in OA rats

The structural integrity of testicular tissue is essential for spermatogenesis, and seminiferous tubule morphology directly reflects the extent of testicular injury in OA rats. This study evaluated key morphological parameters, including seminiferous tubule epithelial thickness, diameter, and area (Figure 2E-H). Compared to the normal group, the busulfan-induced model group exhibited significant reductions in all three parameters, confirming severe testicular structural damage. MG treatment at all doses (15, 30, and 60 mg/kg) partially restored these morphological indices, with the 30 mg/kg group demonstrating the most pronounced recovery in epithelial thickness, diameter, and area. These findings indicate that MG effectively repairs testicular tissue damage and reconstructs a spermatogenesis-supportive microenvironment, providing histological support for its sperm quality-enhancing effects. Notably, the superior efficacy of the 30 mg/kg dose suggests its potential as the optimal therapeutic dosage for testicular repair.

3.1.4 MG Restored busulfan-induced hormonal imbalance in OA rats

This study systematically evaluated the endocrine regulatory effects of MG in OA rats by measuring T, LH, and FSH levels (Figure 2I-K). Experimental data revealed that, compared to the control group, the model group exhibited a significant decrease in serum T levels alongside markedly elevated LH and FSH levels, reflecting characteristic endocrine dysfunction in OA rats. VE intervention notably reduced LH and FSH levels but negatively affected T levels. In contrast, MG treatment demonstrated a clear dose-dependent regulatory effect. The 30 mg/kg dose group showed the most pronounced efficacy, significantly attenuating busulfan-induced elevations in LH and FSH levels and restoring them to near-normal ranges. Although the impact on T levels was relatively limited, a modest upward trend was observed. These results confirm MG's endocrine-modulating properties, with the 30 mg/kg dose exhibiting optimal hormonal regulation.

3.2 Exploration of MG's therapeutic targets for OA using network pharmacology and molecular docking

3.2.1 Prediction of MG targets for OA

To identify potential therapeutic targets of MG for OA, a network pharmacology-based analysis was performed. First, DEGs associated with OA were screened from the GEO database using R (Supplementary Table S4). Additionally, disease-related targets were retrieved from GeneCards, OMIM, and CTD database, yielding 14,011 unique targets after duplicate removal. Next, 153 potential MG targets were predicted using Swiss Target Prediction, TCMSP, and Pharm Mapper (Supplementary Table S5). By intersecting the MG targets with disease-related targets, we identified 125 overlapping genes (Supplementary Table S6), which were proposed as potential therapeutic targets for MG in OA (Figure 3A-B).

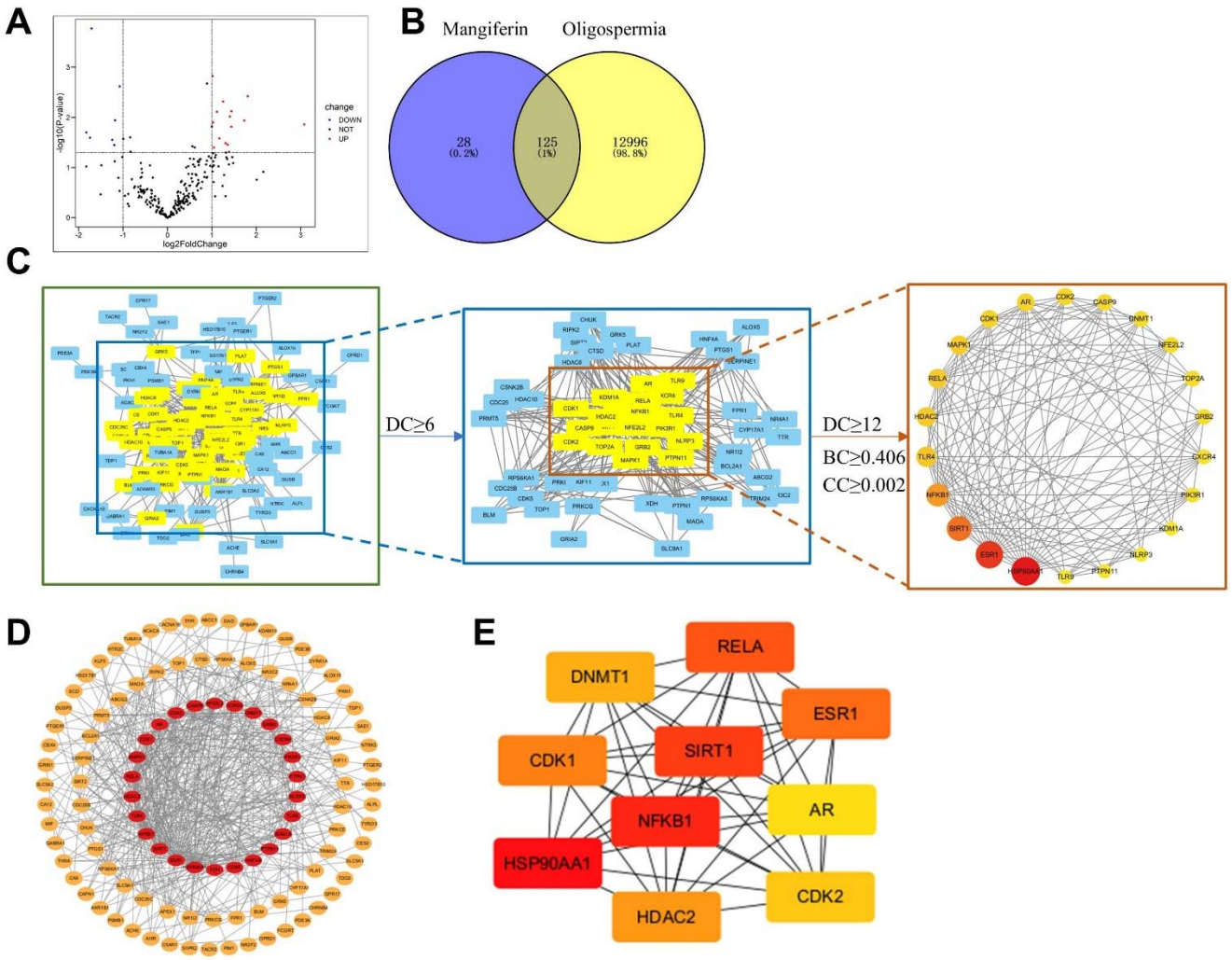

Figure 3. Prediction of the therapeutic targets of MG for oligospermia. (A) The volcano plot showed the differentially expressed genes (DEGs) between oligospermia and normal samples in the GEO database, with significantly upregulated and downregulated genes indicated in red and blue, respectively. (B) The Venn diagram identified 125 targets between MG and OA. (C)The PPI network screened core targets based on DC, CC, and BC. (D) Network analysis further divided targets into core targets (red nodes) and non-core targets (orange nodes). (E) The top 10 hub genes screened by the CytoHubba algorithm were likely to serve as key therapeutic targets.

3.2.2 Screening of core targets via PPI analysis

To further investigate the potential mechanisms of MG in treating OA, the 125 common targets were imported into the STRING database and filtered using a high-confidence threshold (0.700). A PPI network consisting of 113 nodes and 517 edges was constructed. Topological analysis revealed that the median values of DC, CC, and BC were 6, 0.405, and 0.002, respectively. Subsequently, according to the criteria of

DC≥6, CC≥0.405, and BC≥0.002, the core PPI network was screened, and 22 key targets closely related to the therapeutic effects of MG on OA were identified (Figure 3C-D). Using the CytoHubba plugin in Cytoscape 3.10.0 based on the MCC algorithm, 10 hub genes were further screened and identified (Figure 3E), including HSP90AA1, NFKB1, SIRT1, RELA, ESR1, DNMT1, CDK1, HDAC2, CDK2, and AR. Notably, several members of these hub genes, such as NFKB1 and RELA[27], are key transcription factors regulating inflammatory responses, while SIRT1[28] and HSP90AA1[29] are involved in the regulation of oxidative stress responses. In particular, SIRT1, as an important oxidative stress sensor, can regulate cellular redox balance by modulating NAD^+ metabolism. These findings suggest that MG may alleviate OA by concurrently targeting inflammatory and oxidative stress pathways, offering mechanistic insights for further research.

3.2.3 Key pathways screening by functional enrichment analysis

Based on the preliminary results of the PPI network analysis, we initially speculated that MG primarily functioned through anti-inflammatory and antioxidant pathways. To further elucidate its molecular mechanisms, we conducted GO and KEGG enrichment analyses. The GO analysis revealed that the targets of MG were mainly involved in BP such as positive regulation of reactive oxygen species metabolic process, cellular response to hypoxia, and inflammatory responses. In terms of CC, they were primarily enriched in structures like synapses, chromatin, and the cytoplasmic membrane. Regarding MG, they were significantly enriched in key functional domains such as protein kinase activity, ATP binding, and protein binding (Figure 4A). The KEGG pathway analysis further indicated that the mechanisms of MG in treating OA involv pathways related to oxidative stress and inflammatory responses (Figure 4B). Among these, the NOD-like receptor signaling pathway was of significant importance. Within this category of signaling pathways, the NLRP3 inflammasome pathway is the most crucial. This pathway perceives danger signals through the pattern recognition receptor NLRP3, recruits the ASC adaptor protein, and activates Caspase-1. This subsequently cleaves the GSDMD protein, promoting the maturation and release of pro-inflammatory cytokines such as IL-1β, ultimately leading to pyroptosis. This programmed cell death not only directly damages the testicular spermatogenic epithelium but also continuously activates inflammatory responses and oxidative stress, forming a vicious cycle that leads to spermatogenic dysfunction[30].

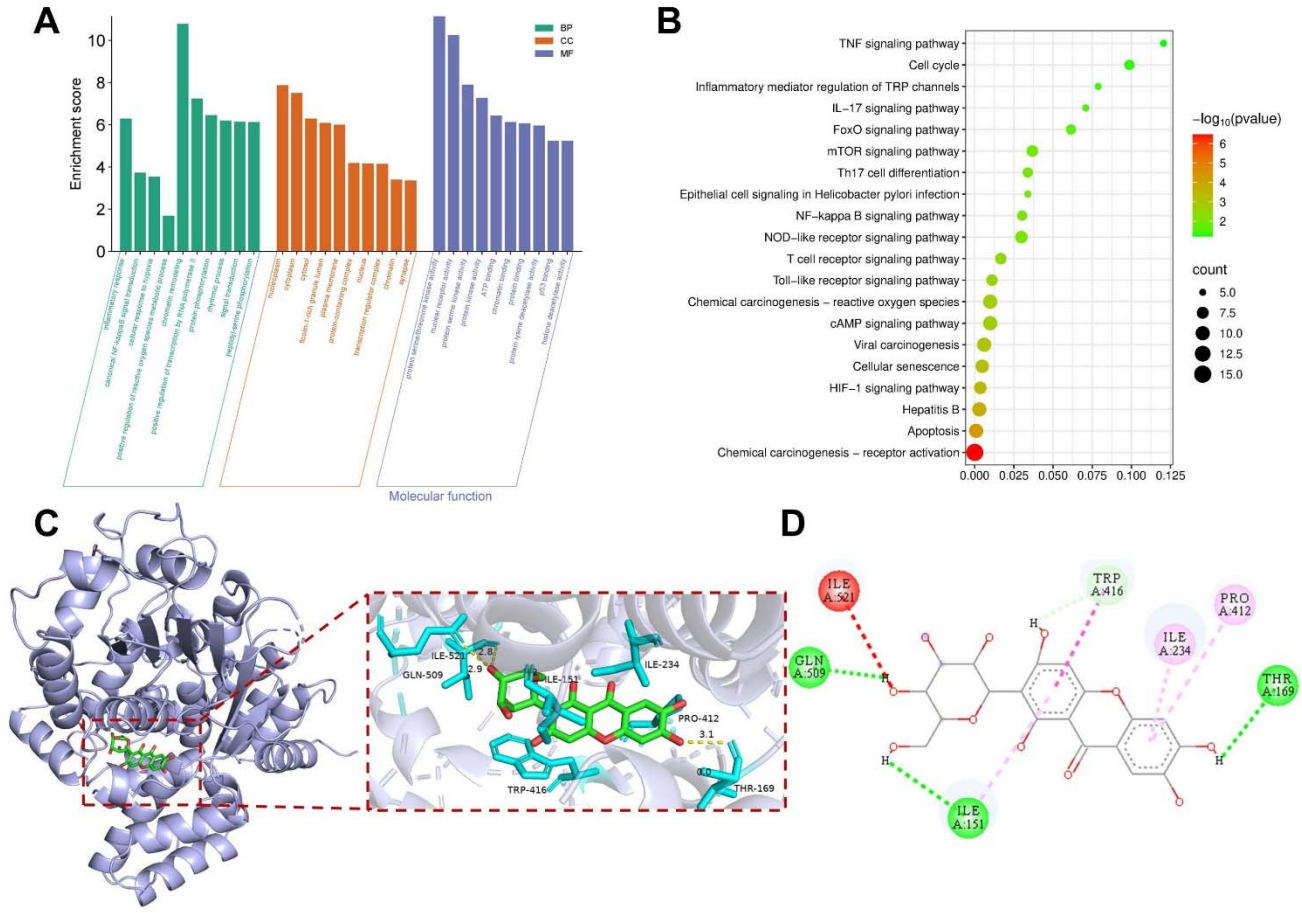

Figure 4. Functional enrichment analysis and molecular docking. (A-B) GO and KEGG predicted key pathways for MG to improve OA. (C) The binding mode of mangiferin with NLRP3 protein was intuitively presented in a three-dimensional structure diagram through molecular docking technology. (D) while the two-dimensional interaction diagram detailed the key binding sites and molecular interactions.

3.2.4 Molecular docking analysis of the binding affinity between ligand (MG) and receptor (NLRP3)

Informed by predictions derived from network pharmacology, it is postulated that MG may exert its reproductive protective effects through the modulation of the NLRP3 inflammasome activation pathway, thereby mitigating pyroptosis. To substantiate this proposed mechanism, we utilized molecular docking techniques to evaluate the binding interactions between MG and NLRP3. The docking analyses revealed that MG exhibits a strong binding affinity with the NLRP3 protein, characterized by a binding free energy of -9.6 kcal/mol, which suggests a stable interaction between the two entities (Figure 4C). Further examination indicated that MG engages in intermolecular interactions with several critical amino acid residues of NLRP3, including ILE-521, GLN-509, ILE-151, TRP-416, ILE-234, PRO-412, and THR-169 (Figure 4D). These interactions may influence the conformation and function of NLRP3. The findings from this structural biology investigation provide significant evidence supporting the direct targeting of the NLRP3 inflammasome by MG, thereby corroborating its mechanism in ameliorating OA through the inhibition of NLRP3 inflammasome activation.

3.3 In vitro and in vivo studies to elucidate the molecular processes of MG in the treatment of OA

3.3.1 MG reduced cell damage in vitro

Benzimidazole (DRB) was employed to produce damage to Sertoli cells for the establishment of an *in vitro* OA model. The CCK-8 assay results (Figure 5A) indicated that DRB intervention markedly decreased cell viability, effectively replicating the pathological condition of OA. Cell viability was greatly enhanced following treatment with MG, with the most effective protective effect noted at a dose of 200 μg/mL (this dose was utilised for future mechanistic investigations). Hoechst staining provided additional indication that MG greatly prevented DRB-induced apoptosis in Sertoli cells (Figure 5B-C).

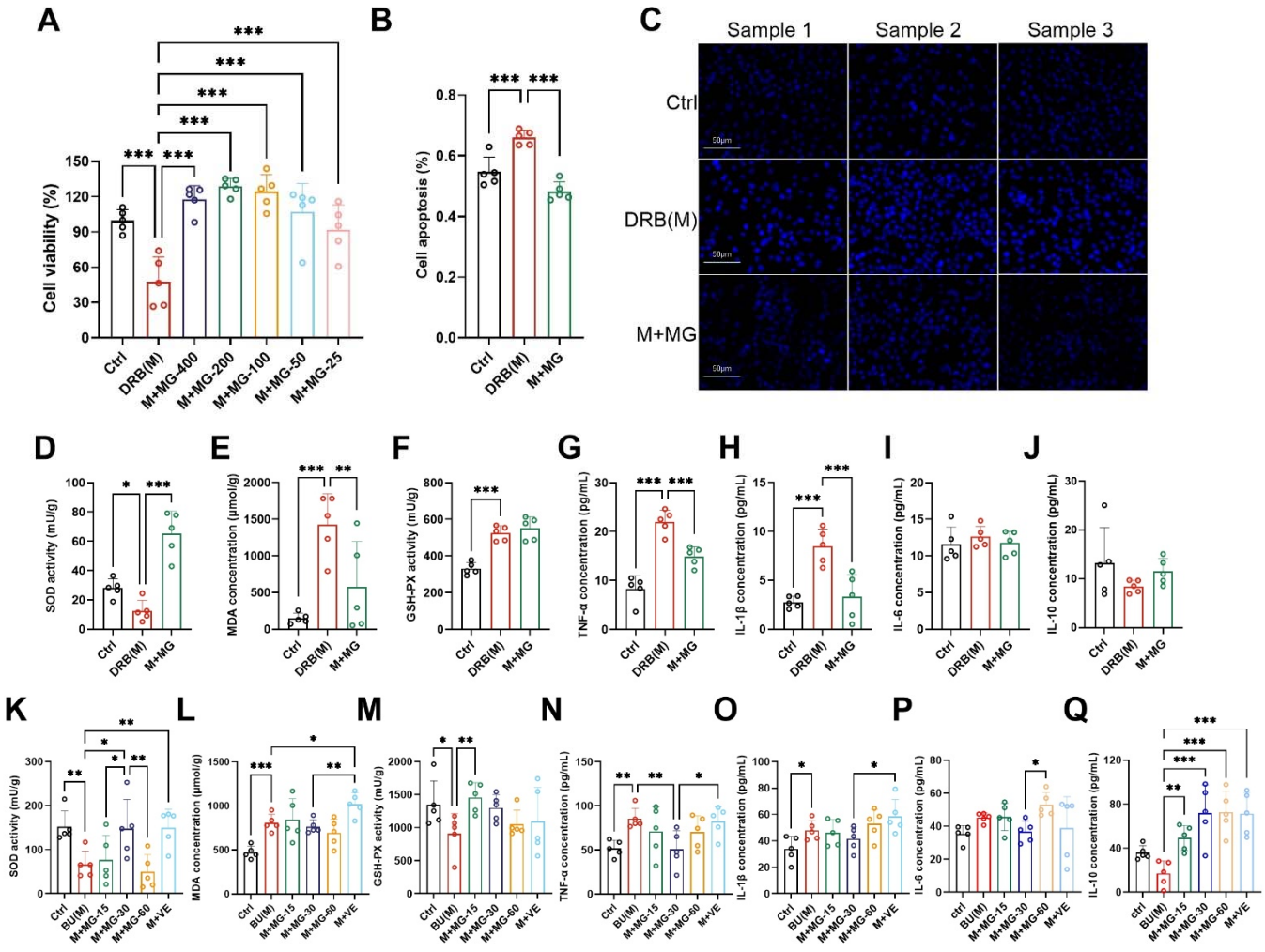

Figure 5. The effects of MG on benzimidazole-induced Sertoli cell damage and oxidative stress/inflammatory responses *in vitro* and *in vivo*. (A) Cell viability detected by CCK-8 assay. (B) Apoptosis levels analyzed by Hoechst 33342 staining. (C) Representative Hoechst staining images (normal cells: light blue; apoptotic cells: bright blue). (D) SOD activity, (E) MDA levels, and (F) GSH-PX activity in Sertoli cells. (G–J) Inflammatory cytokine levels (TNF-α, IL-1β, IL-6, IL-10) in Sertoli cells. (K) SOD activity, (L) MDA levels, and (M) GSH-Px activity in testicular tissue. (N–Q) Inflammatory cytokine levels (TNF-α, IL-1β, IL-6, IL-10) in testicular tissue. Data were presented as Mean ± SD (n=5). *$P < 0.05$, **$P < 0.01$, ***$P < 0.001$.

3.3.2 MG alleviated oxidative stress and inflammatory responses in cell and animal models of OA

KEGG pathway analysis based on network pharmacology predicted that MG treats OA by modulating oxidative stress and inflammatory pathways. This mechanism was experimentally validated *in vitro* and *in vivo*. DRB-induced Sertoli cells demonstrated oxidative stress features, including significantly decreased SOD activity and elevated MDA levels. MG intervention partially restored SOD and MDA levels, though its

impact on GSH-Px was marginal. Inflammatory profiling revealed that DRB markedly upregulated pro-inflammatory cytokines (TNF-α and IL-1β), while MG treatment suppressed their expression. However, MG's effects on IL-6 and IL-10 were less pronounced (Figure 5D-J).

Consistent with *in vitro* data, busulfan-induced OA rats exhibited testicular oxidative stress (reduced SOD/GSH-Px, elevated MDA) and inflammation (increased TNF-α/IL-1β). 30 mg/kg MG administration significantly ameliorated these pathological alterations (Figure 5K-Q). Collectively, these findings demonstrated that MG protected testicular cells by mitigating oxidative damage and attenuating inflammatory responses.

3.3.3 Mangiferin inhibits pyroptosis by suppressing NLRP3 inflammasome activation

Network pharmacology analysis predicted that MG exerts reproductive protective effects by regulating NLRP3 inflammasome-mediated pyroptosis. To validate this hypothesis, we performed molecular experiments (Figure 6). Western blot analysis revealed elevated protein levels of NLRP3, Caspase-1, and GSDMD in Sertoli cells from the model group compared to controls, which were significantly reduced upon MG intervention. RT-qPCR further confirmed these findings, demonstrating that NLRP3, ASC, Caspase-1, and GSDMD mRNA levels were markedly increased in the model group but suppressed by MG. Notably, *in vivo* experiments in OA rats yielded consistent results, with MG downregulating NLRP3 inflammasome-related genes in testicular tissue. These data collectively indicat that MG alleviats oxidative stress and inflammation by inhibiting NLRP3 inflammasome activation and subsequent pyroptosis.

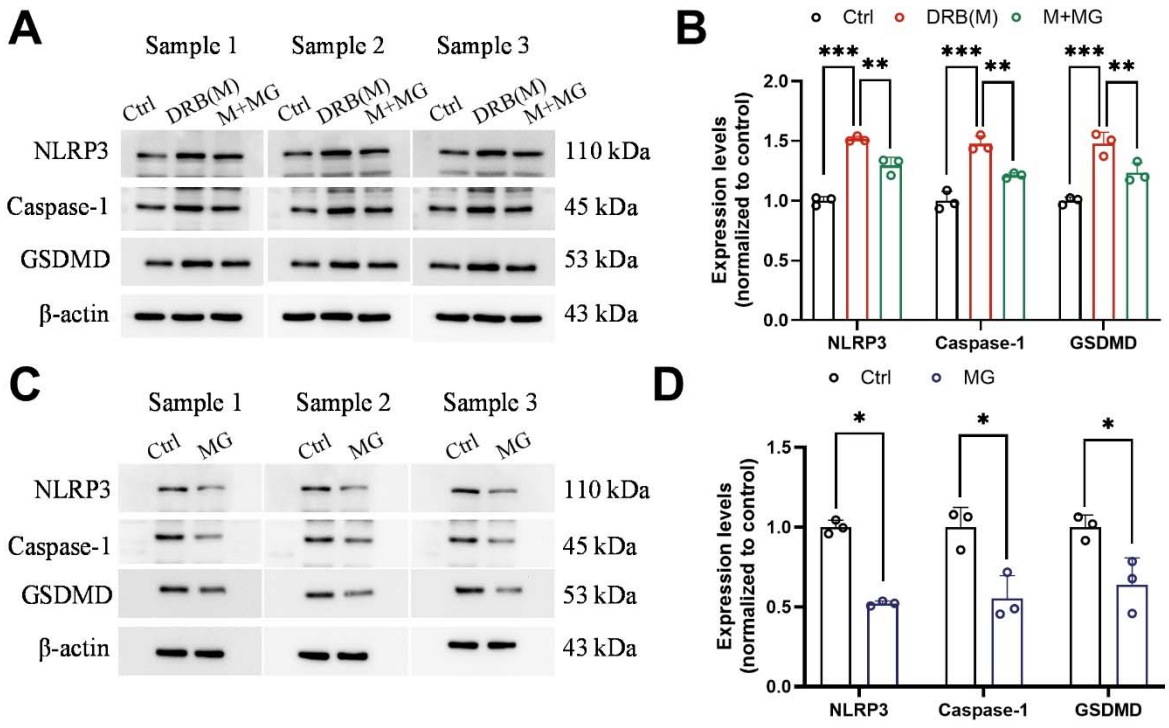

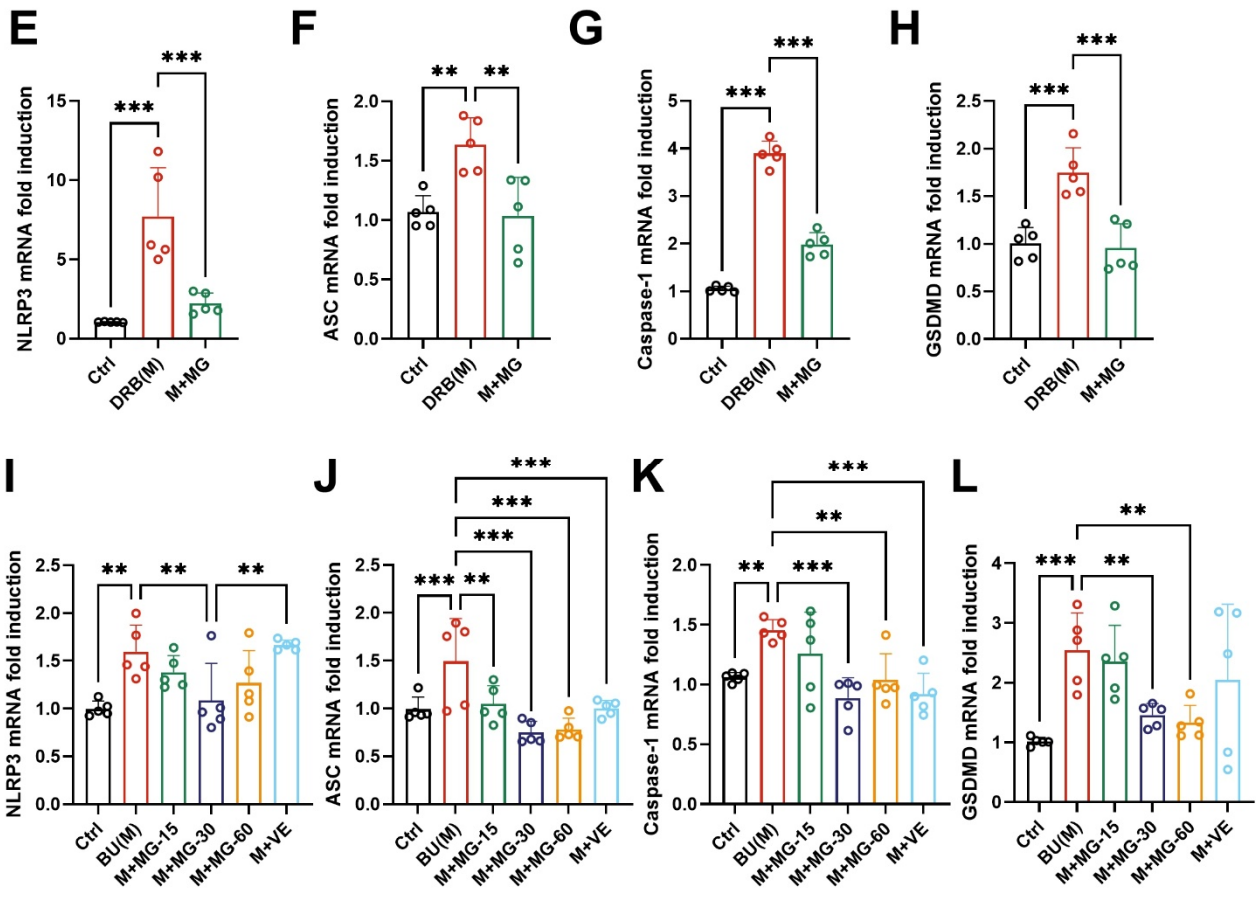

Figure 6. Regulation of the NLRP3 inflammasome signaling pathway by MG in Sertoli cells and OA rats. Western blot was used to determine the protein expression of NLRP3, Caspase-1, GSDMD, and β-actin in the control (Ctrl) group, model group, MG intervention group (M+MG), and Ctrl + MG group. (A and C) Protein immunoblot bands. (B and D) Quantitative analysis of protein expression levels. RT-qPCR was used to detect the mRNA levels of (E) NLRP3, (F) ACS, (G) Caspase-1, and (H) GSDMD in Sertoli cells. (I-L) RT-qPCR analysis of mRNA expression levels of NLRP3, ASC, Caspase-1, and GSDMD in OA rats. Data were presented as Mean ± SD. $^{*}P < 0.05$, $^{**}P < 0.01$, $^{***}P < 0.001$.

Interestingly, even in non-modeled, normally cultured cells, MG slightly reduced NLRP3, Caspase-1, and GSDMD protein expression. These observations suggest that MG, as a natural compound, may not only exert therapeutic effects under pathological conditions but also serve as a safe dietary supplement for maintaining reproductive health.

4. Discussion

OA is a common reproductive disorder affecting approximately 10% of men of reproductive age, characterized by a significant decline in sperm count and quality, often leading to infertility. Existing therapeutic drugs are often associated with notable side effects, thus highlighting the clinical significance of developing novel treatment strategies and elucidating their mechanisms of action. This study is the first to demonstrate that MG significantly improves reproductive function in a rat model of OA induced by busulfan, as evidenced by the regulation of sex hormone levels, enhancement of sperm quality, and alleviation of testicular tissue pathological damage. Through integrated network pharmacology analysis and experimental validation, the study further unraveled the mechanism of action of MG, which involves inhibiting the activation of the NLRP3-ASC-Caspase-1-GSDMD signaling pathway, effectively blocking

the pyroptosis process, thereby reducing inflammatory responses and oxidative stress damage, and ultimately achieving therapeutic effects on OA.

OA is pathologically characterized by reduced sperm count and quality, endocrine dysfunction, and testicular atrophy. The busulfan-induced rat model in this study successfully recapitulated these features[31], including significantly decreased testosterone levels—a key hormone regulating spermatogenesis. Testosterone (T) deficiency impairs Sertoli cell function, by compromising the blood-testis barrier integrity, disrupting sperm adhesion, and hindering apoptotic cell clearance[32]. Additionally, Sertoli cell damage affects FSH signaling, which governs spermatogonial maintenance and differentiation[32]. Consistent with OA pathology, the model group exhibited endocrine dysregulation, including reduced T alongside elevated FSH and LH levels. MG treatment effectively normalized these hormonal imbalances. Histopathological analysis further revealed seminiferous tubule atrophy, epithelial thinning, and extensive Sertoli cell death in model rats, resulting in impaired spermatogenesis and poor sperm quality[33]. In contrast, mangiferin intervention markedly ameliorated these defects, evidenced by restored spermatogenic epithelium thickness, viable Sertoli cells, and improved sperm count and motility. These findings demonstrate that mangiferin alleviates oligospermia by repairing the testicular microenvironment and rebalancing endocrine homeostasis.

Network pharmacology, a pivotal tool in systems biology, enables the systematic prediction of drug mechanisms. Specifically, its predictions indicated that the key hub targets of MG in alleviating OA include SIRT1 and NFKB1. These targets are mainly involved in counteracting mitochondrial oxidative damage, maintaining mitochondrial homeostasis, and suppressing inflammatory responses. Additionally, GO analysis further suggested that MG targets participate in regulating oxidative stress, inhibiting inflammation, and modulating apoptosis. Critically, our experimental validation closely matched these predictions, confirming that MG can mitigate oxidative stress and reduce inflammatory responses. Regarding its antioxidant properties, MG significantly increased SOD activity while reducing MDA levels. This effect likely stems from its direct free radical scavenging capacity and catechol structure, which effectively terminates radical chain reactions[22]. The limited impact on GSH-Px activity suggests that MG's antioxidant mechanism operate independently of the glutathione pathway, or alternatively, reflected temporal variations in antioxidant enzyme system responses. In terms of anti-inflammatory effects, MG exhibited selective inhibition of pro-inflammatory cytokines (TNF-α and IL-1β) rather than IL-6. This specific inhibition pattern aligns with its targeted regulation of the NLRP3 inflammasome pathway. The minimal effect on IL-10 production may indicate selective action on particular immune cell subsets[34,35].

Furthermore, KEGG pathway enrichment analysis predicted several pathways closely related to MG treatment of OA, including the NOD-like receptor signaling pathway, NF-κB pathway, and oxidative stress-related pathways, with the NOD-like receptor pathway being particularly prominent. Subsequently, experimental validation was highly consistent with these predictions. Our experimental validation using western blot and RT-qPCR demonstrated that MG consistently downregulated the NLRP3-ASC-Caspase-1 signaling axis at both protein and mRNA levels, suggesting its potential to suppress NLRP3 inflammasome

activation through transcriptional regulation. Thus, this result directly confirmed the inhibitory effect of MG on the NOD-like receptor signaling pathway as identified in the enrichment analysis. Mechanistically, given the pivotal role of NLRP3 in bridging oxidative stress and pyroptosis, where benzimidazole-induced ROS overproduction activates NLRP3 *via* NF-κB signaling [36], and subsequent NLRP3 inflammasome assembly triggers Caspase-1-dependent GSDMD cleavage, leading to pyroptosis and cytokine release[37]. Our findings reveal MG's dual therapeutic mechanism. It not only directly scavenges ROS to mitigate oxidative stress but also inhibits NLRP3 expression and downstream inflammatory cascades. Notably, MG markedly reduced ASC adapter protein expression. As ASC serves as the essential scaffold for NLRP3 inflammasome formation[38], its downregulation may directly impair NLRP3-ASC-Caspase-1 complex assembly[39], thereby effectively disrupting the pyroptosis signaling pathway. This finding offers novel insights into MG's anti-pyroptotic action.

In addition, network pharmacology analysis suggested that MG regulation of OA also involves energy metabolism pathways, reflected by the close relationship between the identified hub targets and mitochondrial homeostasis, as well as GO molecular functions related to ATP synthesis. Based on this, we propose that MG may influence inflammasome activation through modulation of energy metabolism, thereby implying that its protective effects involve both direct molecular inhibition and metabolic reprogramming. Recent studies have demonstrated that cellular energy metabolism reprogramming plays a pivotal role in NLRP3 priming and activation[40]. The shift from oxidative phosphorylation to anaerobic glycolysis promotes NLRP3 inflammasome assembly and activation[41]. To elucidate the mechanism underlying MG-mediated NLRP3 suppression, we performed targeted energy metabolomics analysis[42] of testicular tissues from oligospermia model rats. Metabolomics data (Figure 7) revealed decreased acetyl-CoA and itaconate levels in the model group, indicating suppressed tricarboxylic acid (TCA) cycle activity[43]. Elevated lactate coupled with reduced glucose-6-phosphate and fructose-6-phosphate suggested metabolic reprogramming toward anaerobic glycolysis[44]. Paradoxically, the concurrent decrease in glycolytic intermediates implied their potential diversion to alternative pathways. Further analysis showed increased 6-phosphogluconate, confirming redirection of glucose-6-phosphate to the pentose phosphate pathway[45]. This metabolic adaptation likely represents a compensatory mechanism to enhance NADPH production for combating oxidative damage[46] in testicular cells, as evidenced by increased oxidative stress markers in oligospermia. Importantly, integrated analysis of targeted metabolomics, molecular pathways, and pharmacodynamics revealed a close link between metabolic reprogramming and therapeutic outcomes. MG treatment restored TCA cycle intermediates (acetyl-CoA) and anti-inflammatory metabolites (itaconate), which were positively correlated with improved sperm quality, elevated serum testosterone, and enhanced oxidative stress markers. This suggests that MG-mediated metabolic remodeling may act as an upstream regulator connecting cellular energy metabolism, pyroptosis inhibition, and hormonal recovery. Activation of the pentose phosphate pathway to restore NADPH metabolism further supports antioxidant capacity, forming a continuous mechanism from metabolic regulation to anti-pyroptotic and reproductive protection. Overall, oligospermia

causes testicular metabolic disturbances, characterized by reduced TCA cycle activity and enhanced glycolysis, which elevate ROS levels and activate the NLRP3 inflammasome. Inflammasome activation damages Sertoli cells, ultimately reducing sperm count, motility, and testosterone levels. MG treatment reverses these metabolic disturbances, inhibits NLRP3-mediated pyroptosis, and restores reproductive function. Building upon these findings, future investigations should systematically evaluate MG's regulatory effects on key metabolic intermediates and elucidate how metabolic reprogramming mechanistically links to NLRP3 inflammasome activation in oligospermia, which may reveal novel therapeutic targets for male infertility.

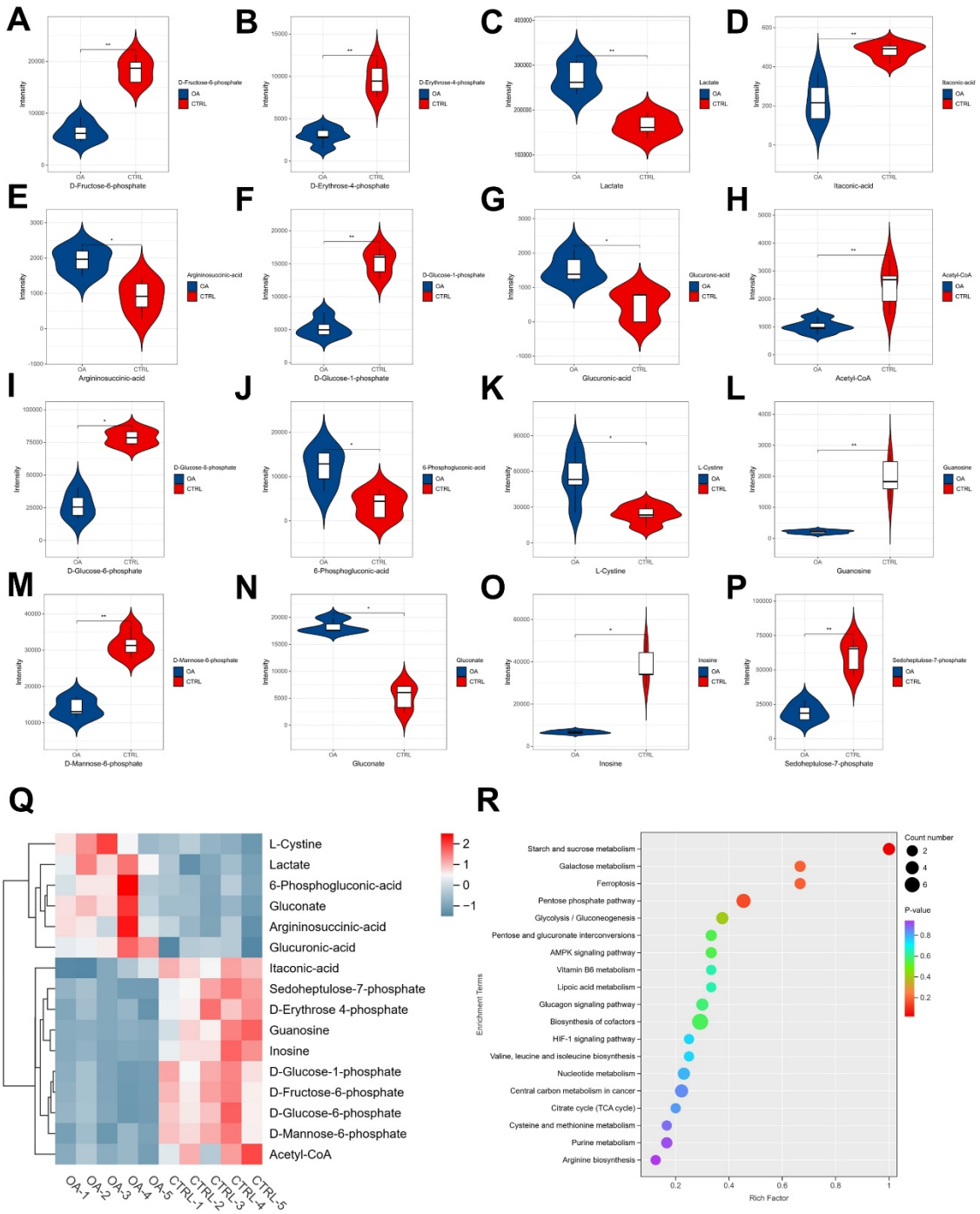

Figure 7. Differential metabolites analysis and KEGG pathway enrichment. (A-P) Violin plots of differential metabolites. (Q-R) Heatmap and KEGG pathway enrichment results of differential metabolites. *$P < 0.05$, **$P < 0.01$, ***$P < 0.001$.

5. Conclusion

Mangiferin showed significant efficacy in improving reproductive function through both *in vivo* and *in vitro* studies. *In vivo* experiments demonstrated its ability to enhance sperm quality, restore sex hormone balance, and mitigate testicular tissue damage. *In vitro* studies confirmed its protective effects on Sertoli cells, including increased viability and suppressed apoptosis. Network pharmacology analysis combined with experimental validation identified NLRP3 inflammasome inhibition as mangiferin's key mechanism, effectively blocking pyroptosis. This dual action not only directly reduced inflammatory responses and oxidative stress but also established a critical negative feedback loop, the attenuated oxidative stress further suppresses NLRP3 activation, creating a self-sustaining cycle of pyroptosis reduction. This unique regulatory mechanism positions mangiferin as a promising candidate for oligospermia treatment and offers novel insights for developing male infertility therapies.

Funding sources

This study was supported by the National Natural Science Foundation of China (NSFC, No. 82301650), the Youth Interdisciplinary Special Fund of Zhongnan Hospital of Wuhan University (Grant No. ZNQNJC2023005), the National Natural Science Foundation of China (NSFC) (Grant No. 82071659) and the General Project of Hubei Provincial Natural Science Foundation (No. 2025AFB936).

Declaration of competing interest

The authors declare that they have no known competing financial interests or personal relationships that could have appeared to influence the work reported in this paper.

Data availability

Data will be made available on request.

References

[1] X. Bai, Y. Tang, Q. Li, Y. Chen, D. Liu, G. Liu, X. Fan, R. Ma, S. Wang, L. Li, K. Zhou, Y. Zheng, Z. Liu, Network pharmacology integrated molecular docking reveals the bioactive components and potential targets of morinda officinalis–lycium barbarum coupled-herbs against oligoasthenozoospermia, Sci. Rep. 11 (2021) 2220. https://doi.org/10.1038/s41598-020-80780-6.

[2] A. Sharma, N. Papanikolaou, S. Abou Sherif, A. Dimakopolou, T. Thaventhiran, C. Go, O. Holtermann Entwistle, A. Brown, R. Luo, R. Jha, A. Prakash, D. Khalifa, H. Lewis, S. Ramaraju, A.R. Leeds, H. Chahal, S. Purkayastha, R. Henkel, S. Minhas, G. Frost, W.S. Dhillo, C.N. Jayasena, Improvements in sperm motility following low- or high-intensity dietary interventions in men with obesity, J. Clin. Endocrinol. Metab. 109 (2024) 449–460. https://doi.org/10.1210/clinem/dgad523.

[3] S. Tommasi, T.H. Kitapci, H. Blumenfeld, A. Besaratinia, Secondhand smoke affects reproductive functions by altering the mouse testis transcriptome, and leads to select intron retention in Pde1a, Environ. Int. 161 (2022) 107086. https://doi.org/10.1016/j.envint.2022.107086.

[4] W. Rodprasert, J. Toppari, H.E. Virtanen, Environmental toxicants and Male fertility, Best Pract. Res. Clin. Obstet. Gynaecol. 86 (2023) 102298. https://doi.org/10.1016/j.bpobgyn.2022.102298.

[5] C.H. Andreassen, R. Holt, L. Juel Mortensen, N.K. Knudsen, J.E. Nielsen, N.N. Poulsen, S.K. Yahyavi, I.M. Boisen, Z. Cui, L. Ongaro, J.P. Hjerresen, B.G. Toft, T. Hasselager, N.R. Jørgensen, D.J. Bernard, A. Juul, C. O'Brien, A. Jørgensen, M.

Blomberg Jensen, Denosumab stimulates spermatogenesis in infertile men with preserved sertoli cell capacity, Cell Rep. Med. 5 (2024) 101783. https://doi.org/10.1016/j.xcrm.2024.101783.

[6] K.C.E. Drechsel, S.L. Broer, H.M.K. Van Breda, F.S. Stoutjesdijk, E. Van Dulmen-den Broeder, A. Beishuizen, W.H. Wallace, D. Körholz, C. Mauz-Körholz, D. Hasenclever, M. Cepelova, A. Uyttebroeck, L. Ronceray, J.W.R. Twisk, G.J.L. Kaspers, M.A. Veening, Semen analysis and reproductive hormones in boys with classical hodgkin lymphoma treated according to the EuroNet-PHL-C2 protocol, Hum. Reprod. 39 (2024) 2411–2422. https://doi.org/10.1093/humrep/deae204.

[7] S.I. Kumalic, I.V. Klun, E.V. Bokal, B. Pinter, Effect of the oral intake of astaxanthin on semen parameters in patients with oligo-astheno-teratozoospermia: a randomized double-blind placebo-controlled trial, Radiol. Oncol. 55 (2020) 97–105. https://doi.org/10.2478/raon-2020-0062.

[8] T. Matsuda, Y. Horii, K. Muguruma, Y. Komatz, O. Yoshida, MicrosurgicalEpididymovasostomy forObstructive azoospermia: FactorsAffecting postoperative fertility, Eur. Urol. 26 (1994) 322–326. https://doi.org/10.1159/000475408.

[9] Y. Wang, X. Fu, H. Li, Mechanisms of oxidative stress-induced sperm dysfunction, Front. Endocrinol. 16 (2025) 1520835. https://doi.org/10.3389/fendo.2025.1520835.

[10] D. Almarzouq, M. Al-Maghrebi, NADPH oxidase-mediated testicular oxidative imbalance regulates the TXNIP/NLRP3 inflammasome axis activation after ischemia reperfusion injury, Antioxidants 12 (2023) 145. https://doi.org/10.3390/antiox12010145.

[11] Z. Rao, Y. Zhu, P. Yang, Z. Chen, Y. Xia, C. Qiao, W. Liu, H. Deng, J. Li, P. Ning, Z. Wang, Pyroptosis in inflammatory diseases and cancer, Theranostics 12 (2022) 4310–4329. https://doi.org/10.7150/thno.71086.

[12] Y.-B. Ruan, X.-H. Liu, J.-Z. Jiang, T. Nie, J. Ma, Leydig cells pyroptosis in testis mediates deoxynivalenol-induced male reproductive toxicity in mice, Sci. Total Environ. 954 (2024) 176432. https://doi.org/10.1016/j.scitotenv.2024.176432.

[13] J. Xu, G. Núñez, The NLRP3 inflammasome: activation and regulation, Trends Biochem. Sci. 48 (2023) 331–344. https://doi.org/10.1016/j.tibs.2022.10.002.

[14] M.E. Ferreiro, C.S. Méndez, L. Glienke, C.M. Sobarzo, M.J. Ferraris, D.A. Pisera, L. Lustig, P.V. Jacobo, M.S. Theas, Unraveling the effect of the inflammatory microenvironment in spermatogenesis progression, Cell Tissue Res. 392 (2023) 581–604. https://doi.org/10.1007/s00441-022-03703-z.

[15] Y. Zhang, M. Shu, S. Shan, H. Liu, Y. Zhang, C. Song, Q. Xu, Y. Fan, C. Lu, Perfluorohexane sulfonic acid disrupts the immune microenvironment for spermatogenesis by damaging the structure of the blood-testis barrier in mice, Adv. Sci. 12 (2025) 2409383. https://doi.org/10.1002/advs.202409383.

[16] S. Jiang, Y. Xu, Y. Fan, Y. Hu, Q. Zhang, W. Su, Busulfan impairs blood–testis barrier and spermatogenesis by increasing noncollagenous 1 domain peptide via matrix metalloproteinase 9, Andrology 10 (2022) 377–391. https://doi.org/10.1111/andr.13112.

[17] S. Yang, G. Huang, J.P.-Y. Ting, Mitochondria and NLRP3: to die or inflame, Immunity 58 (2025) 5–7. https://doi.org/10.1016/j.immuni.2024.12.007.

[18] S.L. Lage, E.P. Amaral, K.L. Hilligan, E. Laidlaw, A. Rupert, S. Namasivayan, J. Rocco, F. Galindo, A. Kellogg, P. Kumar, R. Poon, G.W. Wortmann, J.P. Shannon, H.D. Hickman, A. Lisco, M. Manion, A. Sher, I. Sereti, Persistent oxidative stress and inflammasome activation in CD14highCD16− monocytes from COVID-19 patients, Front. Immunol. 12 (2022) 799558. https://doi.org/10.3389/fimmu.2021.799558.

[19] P. Antonuccio, A.G. Micali, C. Romeo, J. Freni, G. Vermiglio, D. Puzzolo, F. Squadrito, N. Irrera, H.R. Marini, R.A. Rana, G. Pallio, L. Minutoli, NLRP3 Inflammasome: A New Pharmacological Target for Reducing Testicular Damage Associated with Varicocele, IJMS 22 (2021) 1319. https://doi.org/10.3390/ijms22031319.

[20] X. Yang, P. Liu, Y. Cui, M. Song, X. Zhang, C. Zhang, Y. Jiang, Y. Li, T-2 toxin caused mice testicular inflammation injury via ROS-mediated NLRP3 inflammasome activation, J. Agric. Food Chem. 70 (2022) 14043–14051. https://doi.org/10.1021/acs.jafc.2c05317.

[21] L. Yu, M. Wang, S. Guo, Y. Li, L. Zhou, A. Said·Talab, L. Zhang, C. Xue, Y. Wang, T. Zhang, The protective effects of sea cucumber male gonad peptides against testicular damage and spermatogenesis disorder in Male mice, J. Future Foods (2025). https://doi.org/10.1016/j.jfutfo.2025.06.002.

[22] T. Dutta, T. Das, A.V. Gopalakrishnan, S.C. Saha, M. Ghorai, S. Nandy, M. Kumar, Radha, A. Ghosh, N. Mukerjee, A. Dey, Mangiferin: the miraculous xanthone with diverse pharmacological properties, Naunyn-Schmiedeberg's Arch Pharmacol 396 (2023) 851–863. https://doi.org/10.1007/s00210-022-02373-6.

[23] X. Deng, B. Lin, F. Wang, P. Xu, N. Wang, Mangiferin attenuates osteoporosis by inhibiting osteoblastic ferroptosis through Keap1/Nrf2/SLC7A11/GPX4 pathway, Phytomed.: Int. J. Phytother. Phytopharm. 124 (2024) 155282. https://doi.org/10.1016/j.phymed.2023.155282.

[24] S.A. Bisong, I.E. Ukoh, V.U. Nna, P.E. Ebong, Vitamin E attenuates nicotine- and noise-induced reproductive impairment in Male albino wistar rats, Andrologia 50 (2018) e13050. https://doi.org/10.1111/and.13050.

[25] A. Bashamboo, B. Ferraz-de-Souza, D. Lourenço, L. Lin, N.J. Sebire, D. Montjean, J. Bignon-Topalovic, J. Mandelbaum, J.-P. Siffroi, S. Christin-Maitre, U. Radhakrishna, H. Rouba, C. Ravel, J. Seeler, J.C. Achermann, K. McElreavey, Human male infertility associated with mutations in NR5A1 encoding steroidogenic factor 1, Am. J. Hum. Genet. 87 (2010) 505–512. https://doi.org/10.1016/j.ajhg.2010.09.009.

[26] O. Hiort, P.M. Holterhus, T. Horter, W. Schulze, B. Kremke, M. Bals-Pratsch, G.H. Sinnecker, K. Kruse, Significance of mutations in the androgen receptor gene in males with idiopathic infertility, J. Clin. Endocrinol. Metab. 85 (2000) 2810–2815. https://doi.org/10.1210/jcem.85.8.6713.

[27] D. Zhao, L. Wu, X. Fang, L. Wang, Q. Liu, P. Jiang, Z. Ji, N. Zhang, M. Yin, H. Han, Copper exposure induces inflammation and PANoptosis through the TLR4/ NF-κB signaling pathway, leading to testicular damage and impaired spermatogenesis in Wilson disease, (2024).

[28] S. Liang, Y. Yin, Z. Zhang, Y. Fang, G. Lu, H. Li, Y. Yin, M. Shen, Moxibustion prevents tripterygium glycoside-induced oligoasthenoteratozoospermia in rats via reduced oxidative stress and modulation of the Nrf2/HO-1 signaling pathway, Aging (Milano) (2024). https://doi.org/10.18632/aging.205475.

[29] P. Esakky, D.A. Hansen, A.M. Drury, K.H. Moley, Cigarette smoke condensate induces aryl hydrocarbon receptor-dependent changes in gene expression in spermatocytes, Reproductive Toxicology 34 (2012) 665–676. https://doi.org/10.1016/j.reprotox.2012.10.005.

[30] L. Walenta, N. Schmid, J.U. Schwarzer, F.-M. Köhn, H.F. Urbanski, R. Behr, L. Strauss, M. Poutanen, A. Mayerhofer, NLRP3 in somatic non-immune cells of rodent and primate testes, Reproduction 156 (2018) 231–238. https://doi.org/10.1530/REP-18-0111.

[31] R. Pu, J. Liu, A. Zhang, J. Yang, W. Zhang, X. Long, X. Ren, H. Hua, D. Shi, W. Zhang, L. Liu, Y. Liu, Y. Wu, Y. Bai, N. Cheng, Modeling methods for busulfan-induced oligospermia and asthenozoospermia in mice: a systematic review and meta-analysis, J. Assist. Reprod. Genet. 40 (2023) 19–32. https://doi.org/10.1007/s10815-022-02674-y.

[32] L. Li, W. Lin, Z. Wang, R. Huang, H. Xia, Z. Li, J. Deng, T. Ye, Y. Huang, Y. Yang, Hormone Regulation in Testicular Development and Function, IJMS 25 (2024) 5805. https://doi.org/10.3390/ijms25115805.

[33] Z. Jia, S. Liu, T. Chen, Z. Shi, X. Li, Z. Gao, Q. Zhang, C. Zhong, Chlorogenic acid can improve spermatogenic dysfunction in rats with varicocele by regulating mitochondrial homeostasis and inhibiting the activation of NLRP3 inflammasomes by oxidative mitochondrial DNA and cGAS/STING pathway, Bioorganic Chemistry 150 (2024) 107571. https://doi.org/10.1016/j.bioorg.2024.107571.

[34] M. Wang, M. Fijak, H. Hossain, M. Markmann, R.M. Nüsing, G. Lochnit, M.F. Hartmann, S.A. Wudy, L. Zhang, H. Gu, L. Konrad, T. Chakraborty, A. Meinhardt, S. Bhushan, Characterization of the Micro-Environment of the Testis that Shapes the Phenotype and Function of Testicular Macrophages, The Journal of Immunology 198 (2017) 4327–4340. https://doi.org/10.4049/jimmunol.1700162.

[35] W.R. Winnall, M.P. Hedger, Phenotypic and functional heterogeneity of the testicular macrophage population: a new regulatory model, Journal of Reproductive Immunology 97 (2013) 147–158. https://doi.org/10.1016/j.jri.2013.01.001.

[36] M. Sadrkhanloo, M. Entezari, S. Orouei, A. Zabolian, A. Mirzaie, A. Maghsoudloo, R. Raesi, N. Asadi, M. Hashemi, A. Zarrabi, H. Khan, S. Mirzaei, S. Samarghandian, Targeting Nrf2 in ischemia-reperfusion alleviation: From signaling networks to therapeutic targeting, Life Sciences 300 (2022) 120561. https://doi.org/10.1016/j.lfs.2022.120561.

[37] N. Kelley, D. Jeltema, Y. Duan, Y. He, The NLRP3 Inflammasome: An Overview of Mechanisms of Activation and Regulation, IJMS 20 (2019) 3328. https://doi.org/10.3390/ijms20133328.

[38] R. Zhou, A.S. Yazdi, P. Menu, J. Tschopp, A role for mitochondria in NLRP3 inflammasome activation, Nature 469 (2011) 221–225. https://doi.org/10.1038/nature09663.

[39] J. Fu, H. Wu, Structural Mechanisms of NLRP3 Inflammasome Assembly and Activation, Annu. Rev. Immunol. 41 (2023) 301–316. https://doi.org/10.1146/annurev-immunol-081022-021207.

[40] P. Su, X. Mao, J. Ma, L. Huang, L. Yu, S. Tang, M. Zhuang, Z. Lu, K.S. Osafo, Y. Ren, X. Wang, X. Lin, L. Huang, X. Huang, E.I. Braicu, J. Sehouli, P. Sun, ERRα promotes glycolytic metabolism and targets the NLRP3/caspase-1/GSDMD pathway to regulate pyroptosis in endometrial cancer, J. Exp. Clin. Cancer Res. 42 (2023) 274. https://doi.org/10.1186/s13046-023-02834-7.

[41] W.-J. Zhong, T. Liu, H.-H. Yang, J.-X. Duan, J.-T. Yang, X.-X. Guan, J.-B. Xiong, Y.-F. Zhang, C.-Y. Zhang, Y. Zhou, C.-X. Guan, TREM-1 governs NLRP3 inflammasome activation of macrophages by firing up glycolysis in acute lung injury, Int. J. Biol. Sci. 19 (2023) 242–257. https://doi.org/10.7150/ijbs.77304.

[42] R. Li, Q. Zeng, X. Zhang, J. Jing, X. Ge, L. Zhao, B. Yi, J. Tu, T. Fu, J. Wen, J. Shen, Xanthophyll esterases in association with fibrillins control the stable storage of carotenoids in yellow flowers of rapeseed (*brassica juncea*), New Phytol. 240 (2023) 285–301. https://doi.org/10.1111/nph.18970.

[43] Y. Cui, J. Han, J. Ren, H. Chen, B. Xu, N. Song, H. Li, A. Liang, G. Shen, Untargeted LC-MS-based metabonomics revealed that aristolochic acid I induces testicular toxicity by inhibiting amino acids metabolism, glucose metabolism, β-oxidation of fatty acids and the TCA cycle in Male mice, Toxicol. Appl. Pharmacol. 373 (2019) 26–38. https://doi.org/10.1016/j.taap.2019.04.014.

[44] C. Deng, J. Zhang, Y. Huo, H. Xue, W. Wang, J. Zhang, X. Wang, Melatonin alleviates the heat stress-induced impairment of sertoli cells by reprogramming glucose metabolism, J. Pineal Res. 73 (2022) e12819. https://doi.org/10.1111/jpi.12819.

[45] D. Prokai, A. Pudasaini, M. Kanchwala, A.T. Moehlman, A.E. Waits, K.M. Chapman, J. Chaudhary, J. Acevedo, P. Keller, X. Chao, B.R. Carr, F.K. Hamra, Spermatogonial gene networks selectively couple to glutathione and pentose phosphate metabolism but not cysteine biosynthesis, Iscience 24 (2021) 101880. https://doi.org/10.1016/j.isci.2020.101880.

[46] T. TeSlaa, M. Ralser, J. Fan, J.D. Rabinowitz, The pentose phosphate pathway in health and disease, Nat. Metab. 5 (2023) 1275–1289. https://doi.org/10.1038/s42255-023-00863-2.